

Raman modes of the GeS-type orthorhombic phase of PbTe

M. Baleva and M. Momtchilova

Sofia University, Faculty of Physics, 1126 Sofia, Bulgaria

(Received 11 August 1993; revised manuscript received 11 March 1994)

Raman scattering spectra of PbTe films, grown by laser-assisted deposition on a KCl substrate, containing the metastable GeS-type phase of PbTe, are investigated at different temperatures in the range 64–300 K. The Raman-active modes of the orthorhombic GeS-type phase of PbTe are detected in the low-temperature spectra of the films containing the predominantly GeS-type phase. The investigation of films with thick upper layers of the stable Raman-inactive PbTe fcc phase indicates that the Raman spectra of the films at RT are governed by the scattering on uncompensated Te atoms in the undoped samples and by second-order scattering in the doped films.

INTRODUCTION

PbTe, which at ambient conditions crystallizes in a fcc NaCl-type structure, is known to possess two high-pressure (HP) phases, orthorhombic GeS-type and CsCl-type.^{1,2} We have shown that the nonequilibrium techniques for film growth, laser-assisted deposition (LAD) in particular, provide the possibility of growing films with metastable phases from materials possessing such a phase or phases.³ Using LAD we have grown PbTe films with the metastable HP PbTe phases. On the grounds of the structural,³ optical,^{4,5} and photoelectrical⁶ investigations it has been shown that PbTe films grown by LAD represent heterophase junctions between the sublayer with metastable phases and the sublayer with stable fcc phases, as is schematically shown in Fig. 1. The sublayer with metastable phases (d_m in Fig. 1) is thick enough which enables us to study the properties of PbTe metastable phases without applying any hydrostatic pressure.

In a previous work⁷ we have studied the RT Raman scattering from PbTe films containing the GeS phase predominantly and have detected five Raman peaks. The values of the peak frequencies are consistent with those measured by Ves *et al.*⁸ in bulk PbTe at hydrostatic pressure of about 60 kbar. Thus the peaks in the RT Raman spectra were attributed to Raman-active modes of the orthorhombic PbTe phase. Having the orthorhombic PbTe phase in the form of films, not under hydrostatic pressure, we are able to study the Raman spectra at low temperatures (LT). In the present work an investigation of

the LT Raman spectra of doped and undoped films with different thicknesses (of the order of d_m and much higher, $d_r > d_m$) are undertaken. On the grounds of this investigation it is concluded that the peaks seen in our RT spectra as well as in the spectra of a bulk material under hydrostatic pressure⁸ cannot be attributed to first-order Raman scattering on the GeS-type PbTe phase alone. The Raman-active modes of the orthorhombic GeS-type phase are well seen in the LT Raman spectra of the thin films.

SAMPLES AND EXPERIMENT

PbTe undoped and doped with 0.2 and 0.3 mol % Cr, films grown by LAD on (100) KCl substrates are investigated. As has already been mentioned, the films represent heterophase junctions between the metastable phases, grown adjacent to the substrate with a thickness d_m and the stable fcc phase with a thickness d_r (see Fig. 1).³ The thickness d_r of the upper sublayer with the stable monocrystal (100) NaCl-type phase depends on the number of the laser pulses and can reach about 6 μm in our setup for LAD. Two groups of films are studied: (1) Films with thickness $d > d_m$ which means a thick upper layer (d_r) with the stable monocrystal (100) fcc phase. In these films the presence of the metastable phases can be ignored as the penetration depth of the incident light used in the Raman scattering is of the order of 100 \AA , while the thickness of the upper sublayer varies from 1 to 5 μm . (2) Films with thickness d of the order of d_m ($d_m \approx 0.7 \mu\text{m}$).³ The screening action of the fcc phase in these films cannot be entirely avoided. The stable phase always appears after the growth, even in films thinner than d_m , as a result of the relaxation of the metastable phases at the film surface to the stable one. The thickness of the layers with a relaxed fcc phase, estimated from reflection high-energy electron diffraction (RHEED) investigations, is of the order of the electron penetration depth (about 40 \AA), smaller in the doped films.³

The presence of the metastable polycrystal GeS- and monocrystal CsCl-type phases in the films is proved by x-ray and RHEED investigations.³ The lattice constants and the unit-cell volumes V of the different phases in each

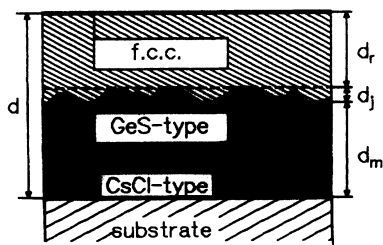


FIG. 1. Schematic representation of the crystal structure over the thickness of the films.

film are determined from the x-ray investigations. From the dependence of the volume changes V/V_0 (V_0 is the volume of the stable fcc phase at pressure $P=0$ kbar and $T=300$ K) on the applied pressure, obtained by Chattopadhyay, Werner, and von Schering¹ and reproduced in Fig. 2, the pressure corresponding to the *as-grown* phases in the different samples are determined. The GeS-type PbTe phase is the only one of the three PbTe phases that has Raman-active modes. The pressure corresponding to the GeS-type phase volume in each sample, discussed in the work, is indicated in Fig. 2 with arrows. The lattice parameters of the GeS-type phase, the corresponding GeS-type phase volumes, and pressures, are given in Table I. In the labeling of the samples, *K* stands for KCl substrate and *T* for PbTe; the notation *CR* means that the samples are doped with Cr and the number after the notation *CR* shows the amount of the dopant (e.g., *CR2* means that the film is doped with 0.2 mol% Cr). In Table I the film thicknesses and the conductivity types are given as well. It is known that undoped PbTe usually grows with excess of Te, which results in *p*-type conductivity. The doping with Cr changes the conductivity to *n*-type, as far as the Cr atoms occupy the Pb vacancies.⁹

Unpolarized Raman spectra are taken as long as the GeS-type phase in the samples under investigation is polycrystalline.³ The Raman scattering is investigated at various temperatures in the range 64–300 K using a nitrogen-cooled cryostat. The spectra are obtained by a SPEX-1404 double-beam monochromator in near back-scattering geometry with spectral resolution 3.1 cm^{-1} . An Ar^+ 514.5-nm laser line with 70 mW is used for excitation. The spectra of samples *CR2K10T* and *CR2K5T* at 64 K are taken at excitation with both 514.5- and 476-nm Ar^+ laser lines. SPEX-1450 tunable excitation filter is used to suppress the laser line background. The samples investigated are highly absorbing in the visible range. Moreover, as it has already been pointed out the orthorhombic GeS-type phase in the samples is screened by the upper Raman inactive fcc phase. Thus an extremely low signal is expected. To detect this signal a sensitive photomultiplier RCA-C31034N with absolute responsivity

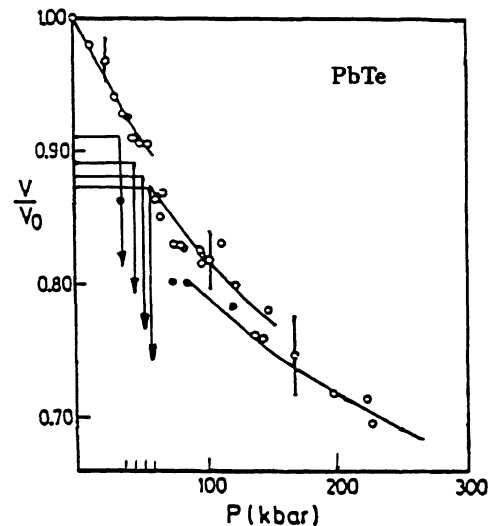


FIG. 2. Pressure-dependent change in the volume of the different PbTe phases, obtained by Chattopadhyay, Werner, and von Schering.¹ The pressures, corresponding to the GeS-type phase in the investigated samples are shown by arrows.

60–70 mA/W in the wavelength range 300–890 nm is used as long as the expected phonon frequencies are close to those of the oxygen rotational Raman lines. To eliminate the air in the Raman lines the samples are placed in a vacuum chamber even when the room-temperature spectra are studied.

The Raman spectra of two thick films—an undoped one (*K217T*, $d=5.6 \mu\text{m}$) and a film doped with 0.3 mol% Cr (*CR3K13T*, $d=1.5 \mu\text{m}$) taken at RT are shown in Fig. 3. Two clearly resolved peaks at 126 and at 143 cm^{-1} are seen in the spectrum of the undoped sample. In the spectrum of the doped sample these peaks are broader and much less intense. Features at about 50 and 100 cm^{-1} are well observable in both spectra. The spectra of the undoped sample taken at different temperatures in the range 64–300 K are shown in Fig. 4. Figures

TABLE I. Sample thickness, conductivity type, and the lattice parameters of the GeS-type phase, determined from the x-ray diffraction. The ratio V/V_0 for the GeS-type phase is calculated from the corresponding lattice parameters and with $V_0=269.3 \text{ \AA}^3$ of the fcc. PbTe volume at $T=300$ K and $P=5$ kbar (Ref. 3). The pressures are determined from the dependence $(V/V_0)(P)$, given in Fig. 2 as it is indicated in the figure by arrows.

Samples	Thickness (μm)	Conductivity type	GeS-type phase lattice parameters (\AA)			GeS-type phase volume changes (V/V_0)	<i>P</i> kbar
			<i>a</i>	<i>b</i>	<i>c</i>		
<i>K217T</i>	5.6	<i>p</i>					
<i>CR3K13T</i>	1.4	<i>n</i>					
<i>CR2K10T</i>	0.9	<i>n</i>	4.684	11.568	4.329	0.87	60
<i>K14T</i>	0.1	<i>p</i>	4.697	11.620	4.345	0.88	50
<i>CR2K3T</i>	0.7	<i>n</i>	4.851	10.890	4.529	0.89	45
<i>CR3K37T</i>	0.7	<i>n</i>	5.048	10.810	4.537	0.91	40

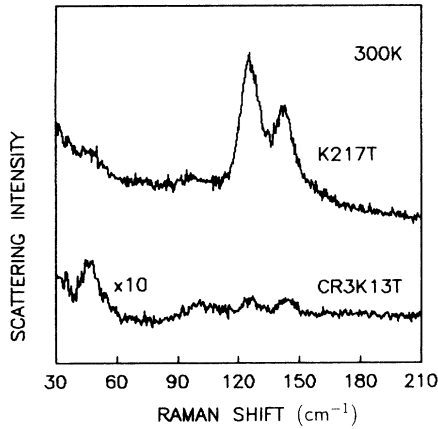


FIG. 3. Raman spectra of (100) monocrystal fcc. PbTe of undoped (*K217T*) and doped with 0.3 mol % Cr (*CR3K13T*) films at room temperature.

5 and 6 represent the spectra of two of the thin films—sample *CR2K3T* and *CR2K10T*, respectively, taken at various temperatures. It is seen from Figs. 5 and 6 that the broad peculiarities in the RT spectra of these thin films split and transform into clearly observed peaks at 64 K. Figure 7 shows the Raman spectra with subtracted Rayleigh scattering of four films at 64 K. The values of the peak frequencies determined from the spectra shown in Fig. 7 are given in Table II.

DISCUSSION

The Raman spectra of the stable NaCl-type PbTe phase—investigation of the thick films

The Raman spectrum of the stable Raman-inactive fcc PbTe phase, obtained from the thick undoped film shown

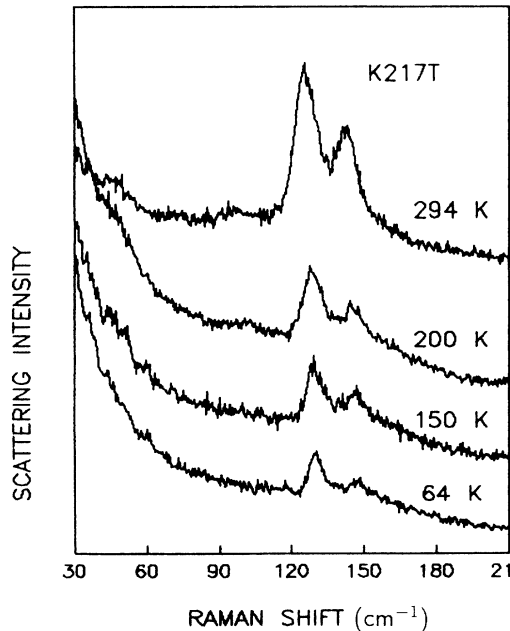


FIG. 4. Raman spectra of (100) monocrystal fcc PbTe phase of the undoped (*K217T*) film taken at different temperatures.

TABLE II. Raman-active modes of the GeS-type PbTe phase. The mode assignment and the frequencies ω_s are obtained from the experimental results of GeS, reported by Vorliček, Gregora, and Chvostova (Ref. 16). The mode frequencies ω_{exp} are obtained from our experimental Raman spectra at 64 K for four samples.

Mode assignment	Samples	Frequencies cm^{-1}				
$4A_g$ (<i>aa</i>)(<i>bb</i>)(<i>cc</i>)	ω_s	18.0	41.0	96.0	108.0	
	ω_{exp}	<i>CR2K10T</i>	13.5	37.5	69.0	84.0
		<i>K14T</i>		36.5	66.5	83.0
		<i>CR2K37T</i>	13.8	37.5	67.5	84.0
$4B_{1g}$ (<i>ab</i>)	ω_s	28.0	42.0	53.0	117.0	
	ω_{exp}	<i>CR2K10T</i>	21.5	45.0	52.5	115.0
		<i>K14T</i>	20.0	43.5	50.0	115.0
		<i>CR2K37T</i>	21.3	45.0	50.0	
$4B_{2g}$ (<i>ac</i>)	ω_s	20.0	85.0			
	ω_{exp}	<i>CR2K10T</i>	20.5	61.0		
		<i>K14T</i>		59.5		
		<i>CR2K37T</i>	18.3	59.5		
$4B_{3g}$ (<i>bc</i>)	ω_s	36.0	105.0			
	ω_{exp}	<i>CR2K10T</i>	29.5	77.0		
		<i>K14T</i>	28.0	74.5		
		<i>CR2K37T</i>	26.5	75.5		
		<i>CR2K3T</i>	28.0	75.0		

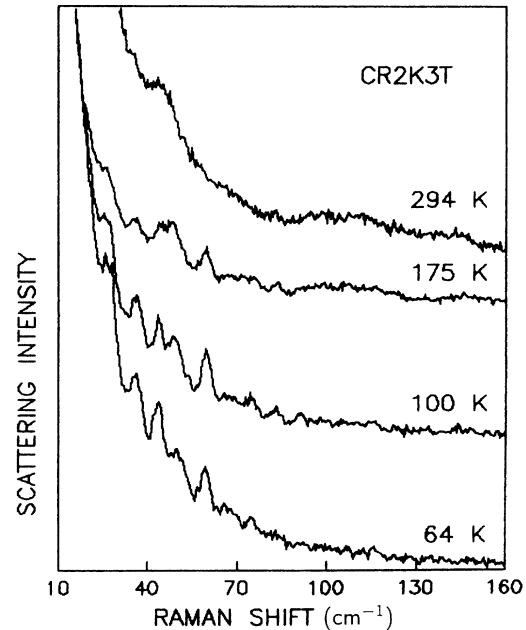


FIG. 5. Raman spectra of thin ($d = 0.7 \mu\text{m}$) film, doped with 0.2 mol % Cr (*CR2K3T*) at different temperatures.

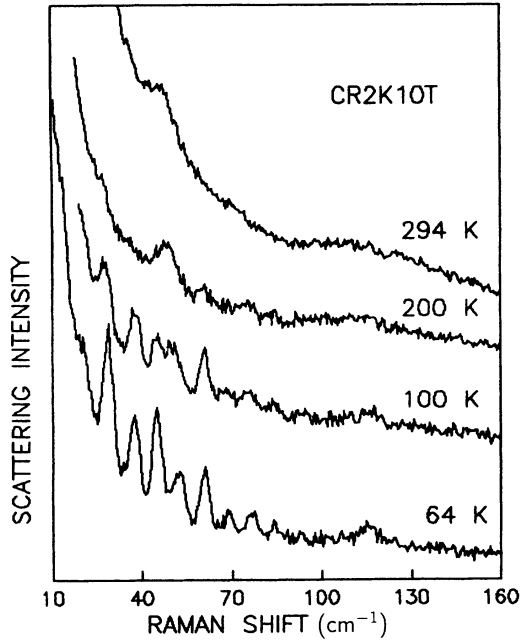


FIG. 6. Raman spectra of thin ($d = 0.9 \mu\text{m}$) film, doped with 0.2 mol % Cr (CR2K10T) at different temperatures.

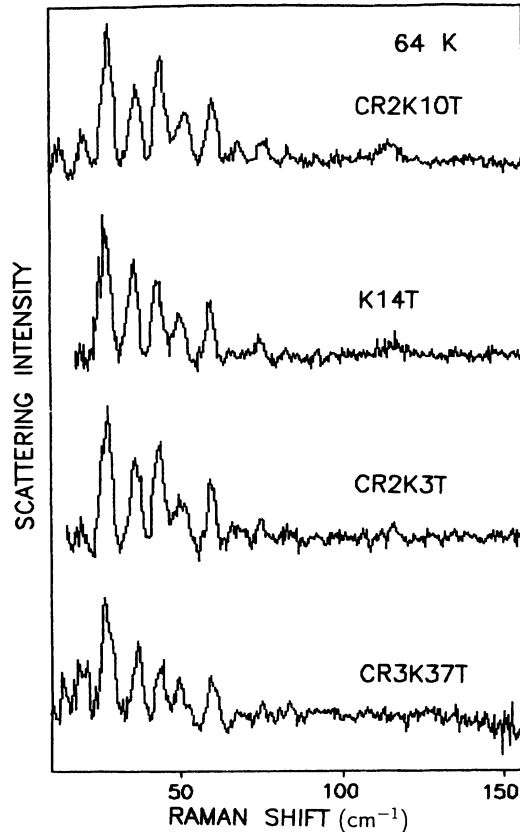


FIG. 7. Raman spectra of films CR3K37T, CR2K3T, K14T, and CR2K10T at 64 K. The Rayleigh scattering is subtracted.

in Fig. 3 (K217T), is very close to the spectra observed on CdTe, GeTe, and $\text{Pb}_{1-2}\text{Sn}_2\text{Te}$ films—with two intense peaks at 126 and at 143 cm^{-1} and a less intense one at about 100 cm^{-1} . The close similarity of these spectra to the spectrum of Te according to Bilz *et al.*¹⁰ indicates that the Raman spectra observed by them on GeTe surfaces are actually due to Te. To verify this statement we have undertaken the following investigations.

(1) The Raman spectra of thick undoped PbTe films with *p*-type conductivity are studied at various temperatures, Fig. 4. The Raman spectra of tellurium have been studied by Pine and Dresselhaus.¹¹ Tellurium crystallizes with space group D_3^4 (or D_3^5) having three atoms per unit cell arranged helically about the *c* axis. The symmetries of the optical phonons at the center of the Brillouin zone are one Raman-active A_1 singlet, one infrared-active (extraordinary ray) A_2 singlet, and two Raman- and infrared-active (ordinary ray) E doublets. Though tellurium is homonuclear, there is dynamic charge associated with A_2 and E modes. Pine and Dresselhaus¹¹ have identified the Raman-active A_1 singlet and two E doublets by the scattering polarization selection rules. Our spectrum at 294 K, shown in Fig. 4, is very similar to the spectrum of Te, taken at the phonon propagation normal to the trigonal Te *c* axis. The difference between our spectrum and that of Pine and Dresselhaus¹¹ is that the peaks in our spectrum are at 124 ± 3.1 and $142 \pm 3.1 \text{ cm}^{-1}$, while the peaks in their spectrum are at 120.4 ± 0.5 and $140.7 \pm 0.5 \text{ cm}^{-1}$. The shift to the higher frequencies, if any, can be attributed to the different distances between the Te atoms in its own unit cell and in the fcc NaCl-type lattice of PbTe. The deficiency of Pb in the PbTe NaCl-type lattice obviously leads to a short-range correlation of the Te atoms in the vicinity of the missing Pb atom analogous to the one in the trigonal Te unit cell. It is also seen from Fig. 4 that the intensities of the most pronounced peaks at 124 and 142 cm^{-1} decrease with the temperature following the Bose-Einstein population factor temperature dependence of the first-order Raman scattering.

(2) The Raman spectra of Cr-doped films of *n*-type conductivity are studied, Fig. 3 (CR3K13T). In these films the Cr atoms occupy the Pb vacancies, compensating in this way for the excess Te atoms.⁹ The comparison of the spectra of the undoped and doped films, shown in Fig. 3, indicates that the peaks at 124 and 142 cm^{-1} , well defined in the undoped film spectrum (K217T), are seen as broad and low intense features in the doped film spectrum (CR3K13T). Then the peaks at 124 and 142 cm^{-1} and the less intense one at about 100 cm^{-1} , seen in a number of telluridies, can be really accounted for by first-order Raman scattering on the uncompensated Te atoms, whose short-range correlation in these compounds is proper to the trigonal Te unit cell.

Apart from the well-defined peaks at 124 and 143 cm^{-1} in the undoped film spectra a feature at about 45 cm^{-1} is well resolved and the feature at about 100 cm^{-1} is broader than in the Te spectrum.¹¹ Features at about 45, 100, 125, and 142 cm^{-1} are seen in the RT Raman spectra of all doped samples. These features quickly disappear on the lowering of the temperature, indicating

second-order scattering. From the one-phonon density of states of fcc PbTe (Ref. 12) and from the selection rules worked out by Burnstein, Johnson, and London¹³ it follows that second-order scattering can be expected at about 45 cm^{-1} [TO+TA photons at Δ direction of the Brillouin zone (BZ) and/or 2TA(Δ)], at about 100 cm^{-1} [LO+LA(X), TO+LA(X), TO+LO(X), and/or 2TA(L)], at 125 cm^{-1} (two-phonon scattering at X point and/or Δ direction) and at 143 cm^{-1} (two-phonon scattering at both L and X points of the BZ).

Thus the Raman spectrum of the undoped PbTe film is governed by the scattering from the uncompensated Te atoms. Second-order Raman scattering is detected in the RT spectra of both doped and undoped samples. In the undoped samples the second-order scattering at about 125 and 143 cm^{-1} is dominated by the more intense scattering on uncompensated Te atoms. To detect the Raman scattering due to the orthorhombic GeS-type PbTe phase the upper two scattering mechanisms have to be excluded. The scattering due to uncompensated Te atoms can be excluded by doping. The second-order Raman scattering can be eliminated to a great extent by lowering the temperature and, which is more important, by reducing the stable fcc phase on the film surfaces to negligible quantities. Then the Raman-active modes of the GeS-type phase can be seen in thin films, with a thickness of the order of d_m , at low temperatures.

Raman-active modes of PbTe GeS-type orthorhombic phase—investigation of thin films

The spectra of two PbTe samples doped with Cr and with thicknesses of the order of d_m (see Fig. 1) are shown in Figs. 5 and 6 at different temperatures. It is seen that the peaks in the spectra become clearly pronounced at temperatures lower than 200 K. The temperature behavior of the spectra can be understood if one takes into account that the upper sublayer with the stable fcc phase is present even in films with thickness $d < d_m$. The surface sublayer with the stable fcc phase is formed during the condensation of the material evaporated by the last laser pulse. The sharp change of the growth conditions may be regarded as a small displacement which returns the pseudoequilibrium state (the metastable phase) with higher free energy to the true equilibrium state (the stable phase). In this way in the sublayer, grown by the last laser pulse, about $100\text{-}\text{\AA}$ thick (the deposition rate is about 100 \AA per pulse), a change of the growth with metastable to stable phase takes place and the stable phase can be regarded as a relaxed metastable phase or, to some extent, as a strained stable fcc phase. The upper stable phase in these films is about 40 \AA thick at RT.³ As the penetration depth of the incident laser light and the escape depth of the scattered light under normal incidence are about 100 \AA in these compounds, it is clear that at RT the upper sublayer will screen the GeS-type phase to a great extent. On the lowering of the temperature, the unit-cell volumes of the phases become smaller and the strained fcc phase obviously transforms back to the adjacent GeS-type phase. In this way the upper sublayer with the fcc phase becomes thinner on the tempera-

ture decrease. At a certain temperature, depending on the upper sublayer thickness, the upper fcc phase transforms entirely into the GeS-type phase. It is seen from Fig. 5 that at temperature about 100 K the stable phase is not already present in film CR2K3T ($d=0.7 \mu\text{m}$); as far as at lower temperatures, the peak intensities decrease. In the thicker film (CR2K10T) ($d=0.9 \mu\text{m}$), where the upper sublayer is thicker, the peak intensities increase to the lowest temperature, indicating in this way the increase of the scattering volume with GeS-type phase up to the lowest temperatures. Thus the increase of the peak intensities in the Raman spectra at LT we account for by the increase of the scattering volume with the Raman-active GeS-type phase, and the peaks seen in the LT spectra can be attributed to the orthorhombic PbTe Raman-active modes. Two of them, those at $22\text{--}25$ and $44\text{--}46 \text{ cm}^{-1}$ are detected in the RT spectra of thin films, reported earlier.⁷ The peculiarity at about 45 cm^{-1} due to second-order scattering, interflows the peaks at 44 and 50 cm^{-1} of the GeS-type phase in the RT spectra. On lowering the temperature, the second-order scattering decreases faster and the peaks at 44 and at 50 cm^{-1} become well resolved at LT (see Figs. 5 and 6). The remaining three peaks, at $123\text{--}127$, at $105\text{--}108$, and at $140\text{--}145 \text{ cm}^{-1}$, seen in the RT spectra of undoped films⁷ as well as in the spectra of a bulk material under hydrostatic pressure,⁸ have to be attributed to scattering on uncompensated Te atoms.

The orthorhombic PbTe phase enters the group of the layerlike type structures, the space group of the lattice is D_{2h}^{16} with four formula units per unit cell. The lattice constants a , b , and c of this phase in the different samples are given in Table I in the setting $D_{2h}^{16} = P_{bnm}$. The GeS-type structure can be viewed as a severely distorted NaCl-type structure with each atom having three strongly bonded neighbors within its own layer and three more distant neighbors, one of which lies in an adjacent layer. The double layers, two per unit cell, are perpendicular to the long axis, b in our setting. The unit cell of a GeS-like compound (after Gashimzade and Kharciev)¹⁴ is shown in Fig. 8. The axes are drawn according to our choice of the setting— P_{bnm} . In Table III the nonequivalent point positions of the Pb and Te atoms in the GeS-type phase unit cell, used in the interpretation of the x-ray diffraction spectra,³ are given.

The center of inversion of the three-dimensional space group D_{2h}^{16} lies between the double layers. The factor-group analysis of the space group D_{2h}^{16} reveals 21 optical and 3 acoustical phonons—7 infrared active and 12 Raman active. The mode frequencies in the orthorhombic PbTe can be obtained by scaling the corresponding frequencies of an orthorhombic A^4B^6 compound. It has been found by Chandrasekhar *et al.*¹⁵ that in the orthorhombic A^4B^6 compounds, such as GeS, GeSe, SnS, and SnSe, the phonon frequencies ω vary according to the relation

$$\omega \sim V^{-0.75} M^{-0.5},$$

where V is the unit-cell volume and M is the sum of the constituent atoms when calculating the low-frequency

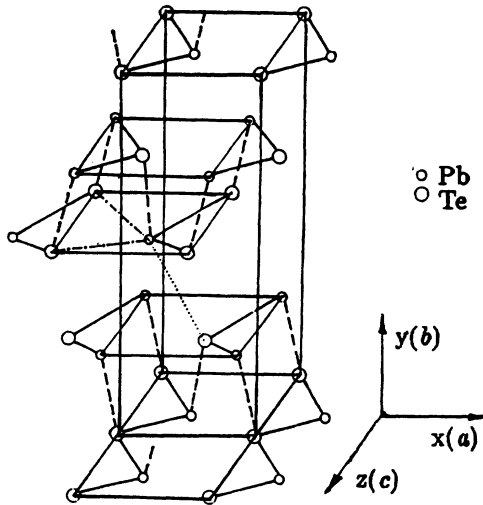


FIG. 8. The unit cell of GeS-like compound (after Ref. 14). The axes are drawn according to the setting P_{bnm} .

modes and the reduced mass for the high-frequency modes. We obtain the mode frequencies ω_s in the orthorhombic PbTe phase from the corresponding frequencies ω (GeS) of GeS, experimentally determined by Vorliček, Gregora, and Chvostova.¹⁶ In the relation

$$\omega_s(\text{PbTe}) = \omega(\text{GeS}) \left[\frac{V_{\text{PbTe}}}{V_{\text{GeS}}} \right]^{-0.75} \left[\frac{M_{\text{PbTe}}}{M_{\text{GeS}}} \right]^{-0.5}, \quad (1)$$

$V_{\text{GeS}} = 167.67 \text{ \AA}^3$, calculated with the GeS lattice parameters and $V_{\text{PbTe}} = 239.26 \text{ \AA}^3$, calculated with the lattice parameters of the GeS-type PbTe phase in sample CR2K3T. The symmetries of the Raman-active modes in the GeS-type PbTe and the scaled values (after Vorliček, Gregora, and Chvostova)¹⁶ of their frequencies are given in Table II together with the values of the peak frequencies obtained from the Raman spectra of four samples at 64 K. The GeS-type phase Raman-active modes of PbTe are tentatively assigned from the comparison of our spectra with the experimental spectrum of GeS, obtained by Vorliček, Gregora, and Chvostova.¹⁶

The GeS-type phase volumes in the investigated samples are different—they correspond to pressures from 40 to 60 kbar (Table I). Nevertheless the peak frequencies differ from sample to sample only within $2\text{--}3 \text{ cm}^{-1}$,

TABLE III. The nonequivalent point positions of the Pb and Te atoms in the PbTe GeS-type phase unit cell.

	x	y	z
Pb	0.500	0.000	0.000
Pb	0.103	0.118	0.250
Te	0.000	0.000	0.000
Te	0.479	-0.145	0.250

which is the setup resolution. Thus we are not able to follow the dependence of the mode frequencies on the pressure or to determine the pressure coefficients $d\omega/dP$ of the modes in this comparatively narrow range of pressure. Moreover, the lattice parameters of the GeS-type phase in the samples are different, making in this way the determination of the dependence of the mode frequencies on the pressure too ambiguous.

CONCLUSION

The LT investigation of the Raman scattering in PbTe films containing the metastable GeS-type phase makes possible the detection of the Raman active modes in the PbTe orthorhombic phase. It is concluded that the upper very thin sublayer with the stable fcc phase screening the GeS-type phase at RT transforms to the metastable phase at LT, leading in this way to an increase of the scattering volume with the Raman-active orthorhombic phase. It is found that three of the peaks in the RT Raman spectra, attributed earlier to the GeS-type phase,^{7,8} are due in fact to scattering on uncompensated Te atoms in the undoped films and to second-order scattering in the films doped with Cr.

The Raman-active modes in the HP GeS-type phase of PbTe, detected here for the first time to our knowledge, are tentatively assigned in accordance with the mode frequencies in GeS, reported by Vorliček, Gregora, and Chvostova.¹⁶

ACKNOWLEDGMENTS

This work has been supported financially by the Ministry of Education and Science under Contract No. Φ -47. The authors are indebted to Dr. I. Ivanov for taking the Raman spectra.

¹T. Chattopadhyay, A. Werner, and H. von Schering, in *High Pressure in Science and Technology*, edited by C. Homan, R. K. Macrone, and E. Whalley, MRS Symposia Proceedings No. 22 (Materials Research Society, Pittsburgh, 1984), p. 93.

²Y. Fujii, K. Kitamura, A. Onodera, and Y. Yamada, *Solid State Commun.* **49**, 135 (1984).

³M. Baleva, L. Bozukov, and E. Tzukeva, *Semicond. Sci. Technol.* **8**, 1208 (1993).

⁴M. Baleva, E. Mateeva, and M. Momtchilova, *J. Phys. Condens. Matter* **4**, 8997 (1992).

⁵M. Baleva and E. Mateeva, *Phys. Rev. B* **48**, 2659 (1993).

⁶M. Baleva, E. Mateeva, M. Petrauskas, R. Tomasiunas, and R. Masteika, *J. Phys. Condens. Matter* **4**, 9009 (1992).

⁷M. Baleva, I. Ivanov, and M. Momtchilova, *J. Phys. Condens. Matter* **4**, 4645 (1992).

⁸S. Ves, A. Yu Pusep, K. Syassen, and M. Cardona, *Solid State Commun.* **70**, 257 (1989).

⁹M. Baleva, *J. Phys. C* **18**, 599 (1985).

¹⁰H. Bilz, A. Bussmann-Holder, W. Jantch, in *Dynamical Properties of IV-VI Compounds*, edited by H. Bilz *et al.*, Springer Tracts in Modern Physics Vol. 99 (Springer, Berlin, 1983), p. 10.

- ¹¹A. S. Pine and G. Dresselhaus, *Phys. Rev. B* **4**, 356 (1971).
- ¹²W. Cochran, A.R. Cowley, G. Dolling, and M. M. Elcombe, *Proc. R. Soc. London* **293**, 433 (1966).
- ¹³E. Burnstein, H. F. Johnson, and R. London, *Phys. Rev.* **139**, A1239 (1965).
- ¹⁴F. M. Gashimzade and V. J. Kharciev, *Fiz. Tverd. Tela* **4**, 434 (1962).
- ¹⁵H. R. Chandrasekhar, R. G. Humphrey, K. Zwick, and M. Cardona, *Phys. Rev. B* **15**, 2177 (1977).
- ¹⁶V. Vorlicěk, I. Gregora, and D. Chvostova, *Phys. Status Solidi B* **116**, 639 (1983).

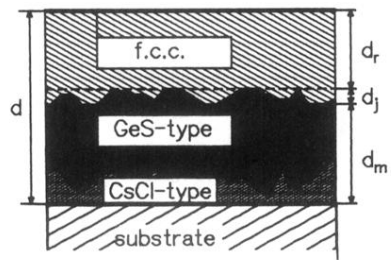


FIG. 1. Schematic representation of the crystal structure over the thickness of the films.